Climate warming effects on grape and grapevine moth (*Lobesia botrana*) in the Palearctic region

Andrew Paul Gutierrez*†, Luigi Ponti*‡, Gianni Gilioli*§ and Johann Baumgärtner*

**Center for the Analysis of Sustainable Agricultural Systems, 37 Arlington Avenue, Kensington, CA 94707, U.S.A.,* †*College of Natural Resources, University of California, Berkeley, CA 94720-3114, U.S.A.,* ‡*Agenzia nazionale per le nuove tecnologie, l'energia e lo sviluppo economico sostenibile (ENEA), Centro Ricerche Casaccia, Via Anguillarese 301, 00123 Rome, Italy and* §*Dipartimento di Medicina Molecolare e Traslazionale, Viale Europa, 11I-25123 Brescia, Italy*

Abstract

1 The grapevine moth *Lobesia botrana* (Den. & Schiff.) (Lepidoptera: Tortricidae) is the principal native pest of grape in the Palearctic region. In the present study, we assessed prospectively the relative abundance of the moth in Europe and the Mediterranean Basin using linked physiologically-based demographic models for grape and *L. botrana*. The model includes the effects of temperature, day-length and fruit stage on moth development rates, survival and fecundity.

2 Daily weather data for 1980–2010 were used to simulate the dynamics of grapevine and *L. botrana* in 4506 lattice cells across the region. Average grape yield and pupae per vine were used as metrics of favourability. The results were mapped using the GRASS Geographic Information System (http://grass.osgeo.org).

3 The model predicts a wide distribution for *L. botrana* with highest populations in warmer regions in a wide band along latitude 40°N.

4 The effects of climate warming on grapevine and *L. botrana* were explored using regional climate model projections based on the A1B scenario of an average +1.8 °C warming during the period 2040–2050 compared with the base period (1960–1970). Under climate change, grape yields increase northwards and with a higher elevation but decrease in hotter areas. Similarly, *L. botrana* levels increase in northern areas but decrease in the hot areas where summer temperatures approach its upper thermal limit.

Keywords GIS, grapevine, PBDM, physiologically based demographic models, population dynamics.

Introduction

The European grapevine moth *Lobesia botrana* (Den. & Schiff.) (Lepidoptera: Tortricidae) attacks host plants in more than 27 families with berry and berry-like fruit over a geographical range that includes Middle Europe, the Mediterranean Basin, southern Russia, Japan, the Middle East, and northern and western Africa (http://www.cabi.org/isc/datasheet/42794) (Venette *et al*., 2003; Thiéry & Moreau, 2005; Maher & Thiery, 2006). *Lobesia botrana* is the most important pest of grape (*Vitis vinifera* L.) in the Palearctic (Savopoulou-Soultani *et al*., 1990), although it also feeds on olive inflorescence (*Olea europaea* L.) (Sciarretta *et al*., 2008). The moth was accidentally introduced and established in Argentina and Chile in South America. It was also introduced to

Correspondence: A. P. Gutierrez. Tel.: +1 510 524 1783; e-mail: casas.global@berkeley.edu

northern California (U.S.A.) where it is considered to have been eradicated using insecticides and pheromone for detection and mating disruption (Varela *et al*., 2010; Heit *et al*., 2015).

Because of its economic importance, several age-stage-structured weather driven models for *L. botrana* have been developed to predict adult flight phenology for field integrated pest management (IPM) decision support (Baumgärtner & Baronio, 1988; Briolini *et al*., 1997; Severini *et al*., 2005; Buffoni & Pasquali, 2007; Ainseba *et al*., 2011; Gilioli *et al*., 2016). Gutierrez *et al*. (2012) linked physiologically-based demographic models (PBDMs) for grapevine (Wermelinger *et al*., 1991) and *L. botrana* and used the system to assess the invasiveness of *L. botrana* in the U.S.A. Prior work linking grapevine and pest models in a Geographic Information System (GIS) context include (Fig. 1): the vine mealybug *Planococcus ficus*, its two parasitoids *Anagyrus pseudococci* and *Leptomastidea abnormis*, and the coccinellid predator *Cryptolaemus*
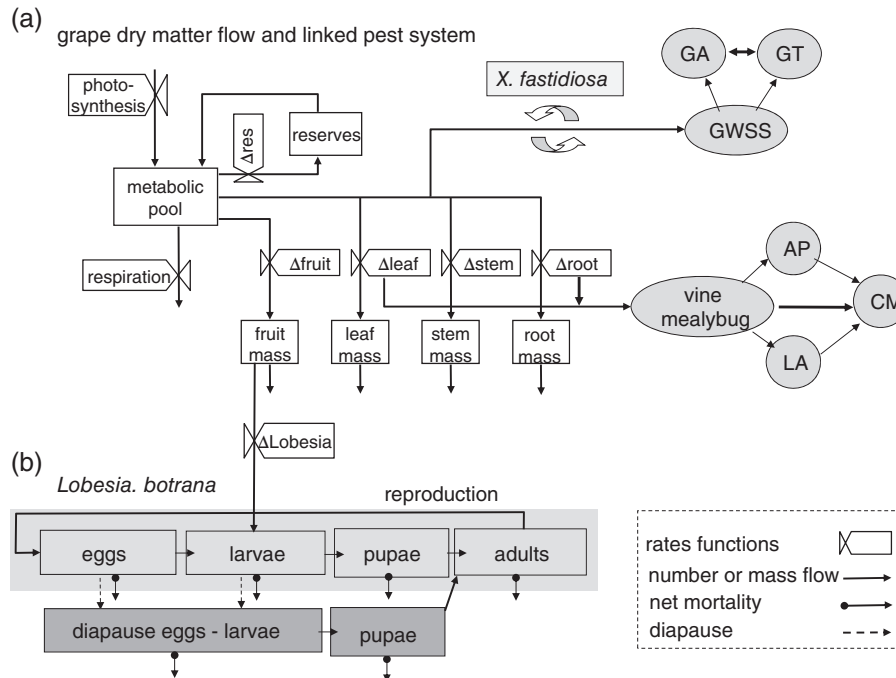
Figure 1 Grapevine-*Lobesia botrana* system. (a) Dry matter flow in grapevine (Gutierrez *et al.*, 1985; Wermelinger *et al.*, 1991) and (b) the linkage of *L. botrana* life-stages including diapause induction and termination (Gutierrez *et al.*, 2012). Note the linkages of two vascular feeding Hemiptera: the vine mealybug and the glassy winged sharpshooter (GWSS) and their natural enemies and the transmission of the Pierce's disease bacterium *Xylella fastidiosa* by GWSS (Gutierrez *et al.*, 2007, 2011).

montrouzieri (Gutierrez *et al.*, 2007), as well as the glassy winged sharpshooter (GWSS) *Homalodisca vitripennis* that vectors the pathogenic bacterium *Xylella fastidiosa* causing Pierce's disease and the two egg parasitoids *Gonatocerus ashmeadi* and *G. triguttatus* that attack it (Gutierrez *et al.*, 2011).

In the present study, the PBDMs for grapevine and *L. botrana* (Gutierrez *et al.*, 2012) were used to analyze the effects of observed weather and a +1.8 °C climate change scenario on the dynamics of the system in the grape growing areas of the Palearctic region of Europe, Eurasia and the Mediterranean Basin.

Materials and methods

The system model for grapevine and L. botrana

A distributed-maturation time population dynamics model (Manetsch, 1976; Vansickle, 1977) (see Appendix) is used to capture the time-varying age-structured dynamics of the subcomponent populations of the grapevine/*L. botrana* system (see below). Biodemographic functions (Gilioli *et al.*, 2016) are used to describe the weather-driven biology of grapevine and *L. botrana* that constitute the *PBDMs* for the species when embedded in the dynamics models. An extant *PBDM* model for grapevine phenology, dry matter growth and development [Wermelinger *et al.*, 1991 (var. *Pinot Noir*); Gutierrez *et al.*, 1985 (var. *Chenin Blanc*)] and a *PBDM* for *L. botrana* (Gutierrez *et al.*, 2012) were used in the present study. Other grape varieties were studied by Gutierrez *et al.* (1985) who found that *Chenin Blanc* had the highest yields, followed closely by *Pinot noir* and *Zinfandel*, with *Cabernet sauvignon* producing 50% of Chenin

Blanc yield. Numerous varieties occur across the Palearctic region, although we use the parameters for *Pinot noir* as the standard. Grape yield also vary with vine age, soil, agronomic practices and other factors (Winkler *et al.*, 1974) and hence our estimates of yield are heuristic. Only a brief description of the grapevine model is given below, whereas the biodemographic functions for *L. botrana* are discussed in detail.

The system model for grapevine and *L. botrana* is modular and consists of 13 {$n = 1, \ldots ,13$} linked age-structured population dynamics models that may be in units of numbers or mass. The grapevine model consists of subunit models for the mass of leaves {$n = 1$}, stem {2}, shoots {3} and root {4} and the mass and number of fruit clusters {5, 6}. The submodels for *L. botrana* consist of age-structured population models for nondiapause and diapause immature stages respectively (e.g. eggs {7, 8}, larvae {9, 10} and pupae {11, 12}) and nondiapause adults {13}. The underpinning modelling concepts are found in Gutierrez and Baumgärtner (1984) and Gutierrez (1992, 1996), whereas the mathematics of the time invariant and time varying distributed maturation-time dynamics model are provided in Manetsch (1976), Vansickle (1977) and DiCola *et al.* (1999). A brief review of the mathematics is given in the Appendix. The model is driven by daily weather (see below) and the time step for each dynamics model is a day of variable length in physiological time units as appropriate for the species and/or stage. The system model was coded in the programming language Borland Delphi Pascal.

Grapevine. The grapevine model captures the phenology of winter dormancy, bud break, veraison and harvest, as well
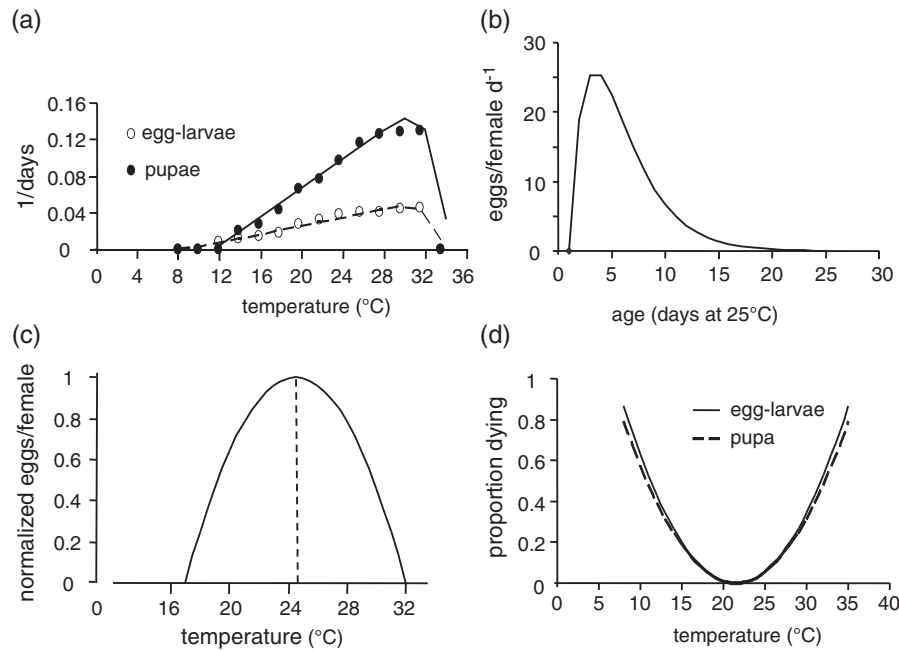
Figure 2 The thermal biology of *Lobesia botrana*. (a) The rate of development of the egg-larval (O) and pupal (●) stages on temperature (data from Brière & Pracros, 1998), (b) the per capita oviposition profile on female age in days at 25 °C (data from Baumgärtner & Baronio, 1988), (c) the effects of temperature on normalized gross fecundity (data from Gabel, 1981) and (d) the proportion dying during the egg-larval and pupal periods on temperature (computed from Briolini *et al.*, 1997). All functions are fits to data from the literature (Gutierrez *et al.*, 2012).

as the dry matter growth and development of vegetative and fruit subunits. The production and allocation of dry matter in grapevine is depicted in Fig. 1(a), whereas the flow via feeding to *L. botrana* is illustrated in Fig. 1(b). Water (irrigation) and nutrients are assumed to be nonlimiting and hence only daily maximum–minimum temperature and solar radiation (MJ/m²/day) drive developmental and dry matter growth of the vine model. The lower thermal threshold for grapevine is 10 °C. Full details of the grapevine model are provided in Wermelinger *et al.* (1991; see also Gutierrez *et al.*, 1985) and hence the model is not reviewed further.

The top-down effect of *L. botrana* feeding on dry matter allocation and growth in grapevine is small, although the economic damage caused by larval grazing on maturing berries may be large and possibly be exacerbated by the action of the grey mold fungus *Botrytis cinerea* (Sclerotiniaceae) (Savopoulou-Soultani & Tzanakakis, 1988) that increases with *L. botrana* infestation levels (Fermaud & Giboulot, 1992). A mechanistic model for *B. cinerea* on grapevine was recently reported by González-Domínguez *et al.* (2015) that accounts for conidia production on various inoculum sources and for multiple infection pathways. Using discriminant function analysis, the ability of the model to predict mild, intermediate and severe epidemics of *B. cinerea* was evaluated. The effects of *Botrytis* are not included in the model, although the model of González-Domínguez *et al.* (2015) can be added to our grapevine system model.

Important bottom-up plant effects on *L. botrana* include the phenology and abundance of fruit stages and their effects on larval-pupal developmental rates and on adult fecundity and longevity (see below).

The biology of L. botrana *on grapevine.* *Lobesia botrana* over-winters as diapausing pupae in the crevices of vine bark, with adults emerging in spring during a period that overlaps with the development of grapevine inflorescence. Two to three generations occur per year in most areas of Europe with a partial or complete fourth generation accruing in warmer areas (Tzanakakis *et al.*, 1988). Four and five generations occur in hotter areas of Spain (Martin-Vertedor *et al.*, 2010). Larvae of the first generation damage grapevine inflorescences, with those of subsequent generations damaging green, ripening and mature berries. In late summer and autumn, *L. botrana* produces diapause pupae that overwinter and complete development the next spring, when they emerge as new adults (Deseö *et al.*, 1981).

Biodemographic functions describe the developmental rates and fecundity as affected by temperature and larval diet (berry stage), diapause induction and termination, and temperature-dependent mortality (Thiéry *et al.*, 2014). Age-specific mortality as a result of temperature and other factors occurs in all life stages. The data from the literature used to formulate and parameterize the biodemographic models were of varying levels of completeness, and re-interpretation of some of the data was required. Most of the functions were first reported by Gutierrez *et al.* (2012) and are reproduced here for completeness (Fig. 2).

Biodemographic functions for L. botrana *(Gutierrez* et al.*, 2012)*

The model can be developed using proportional rate of development but, for ease of field applications, time (*t*) in the model is chronological days (*d*), whereas age and most rates

in the biodemographic functions are in physiological time units (see below).

Rate of development. Development (aging) within a stage and the transitioning between life stages (e.g. larvae to pupae) is not only temperature-dependent, but also may be influenced by larval diet. Data on the developmental times in days for the pre-imaginal stages reared on artificial diet at several temperatures were reported by Gabel (1981), Savopoulou-Soultani *et al.* (1996) and Brière and Pracros (1998). The extensive data on egg-larval and pupal development in Brière and Pracros (1998) were used to estimate the developmental rate at temperature *T*. We aggregated the egg-larval data to reduce the variability introduced by the fact that a daily observation interval at higher temperatures is long relative to the developmental times of the egg stage. Parsimonious Eqn (1) (*cf* Brière *et al.*, 1999) was fitted to the developmental rate data $R_s(T) = 1/d(T)$ at temperature *T* for the egg-larval (subscript *e-l*) and pupal (*p*) stages (s = *e-l*, *p*), where $d(T)$ is the average developmental time in days (*d*) on diet at temperature *T* (Fig. 2a):

$$R_s(T) = \frac{a(T - \theta_L)}{1 + b^{T - \theta_U}} \qquad (1)$$

$$R_{e-l}(T) = \frac{0.00225(T - 8.9)}{1 + 5^{T - 33}} \qquad (1i)$$

$$R_p(T) = \frac{0.00785(T - 11.5)}{1 + 4.5^{T - 33}} \qquad (1ii)$$

The variables θ_L and θ_U are the lower and upper thermal thresholds, whereas *a* and *b* are constants. Specifically, θ_L and θ_U for the *e-l* stage are 8.9 and 33 °C, respectively (Eqn (1i)), whereas values for the pupal stage (*p*) are 11.5 and 33 °C (Eqn (1ii)). The upper threshold θ_U is approximately the temperature where the function begins declining to zero. Data on adult female longevity were available only at 25 °C (Baumgärtner & Baronio, 1988) and, assuming the developmental thresholds for pupae, the adult developmental rate is scaled as $R_{adult}(T(t)) = 0.77R_p(T(t))$ (Gutierrez *et al.*, 2012). On artificial diet, $R_s(T(t))$ is the proportion of development of a stage that occurs at temperature $T(t)$ at time *t* and, hence, for individuals entering stage *s* at age $x = 0$ at time $t = t_0$, development on average is completed when $\sum_{t_0}^{t} R_s(T(t)) = 1$. In the model, developmental times of cohort members have a characteristic mean and distribution (Fig. A1b).

Developmental times in degree days $[\Delta_s(diet) = d(T) \cdot (T - \theta_L)]$ on artificial diet were computed for all stages in the linear range of $R_s(T)$: eggs $(\Delta_e = 80.1 dd_{>8.9°C})$, larvae $(\Delta_l = 317.2 dd_{>8.9°C})$, pupae $(\Delta_P = 128.5 dd_{>11.5°C})$ and adult longevity $(\Delta_A = 166.8 dd_{>11.5°C})$ (Table 1). During late summer to autumn, increasingly, larvae developing on mature berries become diapause pupae that have an approximately 15% lower mean developmental time in spring compared with nondiapause pupae (i.e. $\Delta_{diap} = 0.85\Delta_p$) (Gutierrez *et al.*, 2012).

Larval and pupal developmental times on diet differ from field values, which vary with host fruit stage (*frt*) (Savopoulou-Soultani *et al.*, 1999; Torres-Vila *et al.*, 1999).

Table 1 Parameters for the *Lobesia botrana* model

Developmental time on mature berries

Eggs ($dd > 8.9$ °C)	80.1 dd
Larvae ($dd > 8.9$ °C)	317.2 dd
Pupae ($dd > 11.5$ °C)	128.5 dd
Adults ($dd > 11.5$ °C)	166.8 dd
Diapause pupae ($dd > 11.5$ °C)	115.0 dd
Sex ratio	1♀:1♂
Delay parameter	25

Scalars for the effects of berry stage on

Berry stage	Larval development time	Pupal development time	Fecundity
Inflorescence	1.25	1.19	0.38
Green berry	1.19	1.14	0.41
Maturing fruit	1.0	1.0	1.0

As a standard, larval and pupal times on mature berries are approximately 10% shorter than on diet (Gabel & Mocko, 1984) (see Supporting information, File S1) and average larval developmental times on inflorescence and green berries are 1.25- and 1.19-fold longer than on mature berries, whereas those for pupae are 1.19- and 1.14-fold longer (Table 1). Hence, in the model, the corrections $[\varphi_l(frt)]$ for larval developmental times on inflorescence, green berries and mature berries are 1.125 (= 0.9 × 1.25), 1.07 (= 0.9 × 1.19) and 0.9, respectively, and those for pupae $[\varphi_p(frt)]$ are 1.07, 1.026 and 0.9. The within season changes in stage developmental times are easily accommodated using the time-varying form of the distributed maturation-time population dynamics model (Vansickle, 1977) (see Appendix).

Ignoring the time variable *t*, the daily increment of aging $[\Delta x_s(T, frt)]$ of larval and pupal stages (subscript *s* = *l, p*) in *dd* at temperature *T* is:

$$\Delta x_s(T, frt) = \varphi_s(frt) \cdot R_s(T) \cdot \Delta_s(diet), \qquad (2i)$$

whereas ageing in the egg and adult stages depends only on temperature (Eqn (2ii)):

$$\Delta x_s(T(t)) = R_s(T(t)) \cdot \Delta_s(diet). \qquad (2ii)$$

Note that $R_s(T(t))$ in Eqns (2i) and (2ii) corrects for the nonlinearity of development with *T* and further changes in physiological time are not always equal to the change in age [i.e. $\Delta t(T(t)) = (T(t) - \theta_L) \geq \Delta x(T(t)) \geq \Delta x(T(t), frt)$]. Lastly, average temperatures in the grape canopy are approximately 3.7% lower than ambient (*cf* Potter *et al.*, 2013).

Reproduction. Observed average per capita fecundity ranges from 120 eggs on grapevine to 170 on an artificial diet, although higher fitness may occur on some wild hosts (e.g. the evergreen shrub *Daphne gnidium* L.) in the Mediterranean region (Thiéry & Moreau, 2005; Maher & Thiery, 2006). Per capita age-specific oviposition rate on grapevine [$eggs\ female^{-1} d^{-1} = F(t, x, T, diet_l)$] (Eqn (3i)) varies with

female age (x) (Baumgärtner & Baronio, 1988) (Fig. 2b), temperature (T) (Gabel, 1981) (Fig. 2c) and the diet (i.e. fruit stage) of the larvae producing the adult female (Savopoulou-Soultani *et al.*, 1999; Torres-Vila *et al.*, 1999; Moreau *et al.*, 2016). We characterize the per capita age-specific fecundity profile [$f(x)$] of adults of age x at 25 °C using the function proposed by Bieri *et al.* (1983), the effect of temperature on fecundity is captured by a concave function [$0 \le \phi(T(t)) \le 1$] in the favourable range [$T_{min} = 17^\circ C$, $T_{max} = 32^\circ C$] and the effects of fruit stage are captured by the step function $\psi(frt)$ (Table 1; Gutierrez *et al.*, 2012).

$$F\left(x, t, T, frt_1\right) = \psi\left(frt, t\right) \cdot \varphi\left(T(t)\right) \cdot f(x), \qquad (3i)$$

where

$$f(x) = \frac{28.5\,(x-1)}{1.5^{x-1}} \; at \; T = 25^\circ C$$

$$\varphi(T(t)) = 1 - \left[\frac{\left(T - T_{min} - T_{mid}\right)}{T_{mid}}\right]^2,$$

$$with \; T_{mid} = \left(T_{max} - T_{min}\right)/2 = 7.5^\circ C.$$

$$\psi\left(frt_1\right) = \begin{cases} 0.31 \; (inflorescence) \\ 0.48 \; (green\;berries) \\ 1 \; (maturing\;fruit) \end{cases}.$$

Sex ratios (sr) vary widely on different hosts with 0.82:1.18 (♀:♂) and 1.02 : 0.98 (♀:♂) reported using stock culture insects raised on artificial diet supplied with plant material from grape varieties *Cabernet sauvignon* and *Red Bacco*, respectively (Thiéry & Moreau, 2005). In a similar study, Thiéry *et al.* (2014) found a 1 : 1 ratio on six varieties of grape. We use $sr = 0.5$ in the model; hence, the total egg-load [$E(t, T, diet_1)$] by all females of age $x = 0$ to x_{max} at time t is:

$$E\left(t, T, frt_1\right) = sr \int_{x=0}^{x_{max}} N(x, t)\, F\left(x, t, T, frt_l\right) dx, \qquad (3ii)$$

where $N(x,t)$ is the number of adults of age x at time t. The eggs are deposited singly in berry clusters, and the adult search for oviposition sites is imperfect and affects realized fecundity. This search behaviour is captured by the functional response model (Eqn (A2)).

Temperature-dependent mortality. The total mortality during the egg-larval and pupal stages varies with temperature (T) (Fig. 2d) (Eqn (4i)), with data from Briolini *et al.* (1997):

$$0 \le \mu_s(T) = c_s \left(\frac{T - T_m}{T_m}\right)^2 \le 1 \qquad (4i)$$

The constants in Eqn (4i) are: $T_m = 21.5\,^\circ C$ and c_s = $\begin{cases} 2.2 \; for\;eggs\;and\;larvae \\ 2.0 \; for\;pupae\;and\;adults \end{cases}$.

In the model, we must convert the stage mortality rate $\mu_s(T)$ to a daily mortality rate [$\Delta\mu_s(T(t))$] and hence we multiply by the proportion of the stage completed during time t:

$$0 \le \Delta\mu_s(T(t)) = \mu_s(T(t))\; \frac{\Delta x_s(T(t))}{\Delta_s(t)} \le 1 \qquad (4ii)$$

Andreadis *et al.* (2005) estimated the super cooling point for diapause and nondiapause pupae as −24.5 and −22.5 °C, respectively, although most pupae die at subzero temperatures well above the super cooling point. Hence, in the absence of sound data, we assume the same mortality rate on temperature for both pupal forms.

Other sources of mortality. Extrinsic mortality occurs as a result of generalist natural enemies, host stage suitability, larval dispersal and other factors, although field life-table data to estimate these factors for *L. botrana* are generally unavailable. In heavily parasitized vineyards, larval mortality during spring/summer may reach 80% and up to 90% mortality may occur during pupal diapause (Marchesini & Dalla Montà, 1994; Xuéreb and Thiéry 2006). Gabel and Roehrich (1995) showed a bimodal pattern in berry stage preference for feeding, with intermediates stages being unsuitable for larval survival. Torres-Vila *et al.* (1997) found that dispersal distance in *L. botrana* larvae increased with larval density, although the mortality rates were the same. Gilioli *et al.* (2016) estimated mortality rates in *L. botrana* using unpublished field population dynamics data and the Manly (1989) simulation estimation approach, although the results are time and place specific, and sampling errors from various sources affected the field data. Lanzarone *et al.* (2017) used Bayesian methods to estimate the mortality using the same data and, although the fits were better, the method requires field data to implement and hence is not general. Hence, to keep larval populations within relative bounds (< 70 larvae per vine), we used a variant of the Nicholson and Bailey (1935) model, where ignoring the time variable t, the aggregate extrinsic mortality [$0 < \mu_c(\cdot) < 1$] is assumed to increase with both temperature [i.e. $\Delta t(T) = dd_{>8.9\,°C}$] and pest density ($N_{eggs} + N_{Larvae}$) but at a decreasing rate (Eqn (5)).

$$0 \le \mu_c(\cdot) = 1 - e^{-0.0002\Delta t(T)\left(N_{eggs} + N_{larvae}\right)} < 1 \qquad (5)$$

The constant 0.0002 is arbitrary and when multiplied by $\Delta t(T)$ estimates the fraction of the population that may be found at temperature T. Thus, $\mu_c(\cdot)$ affects egg-larval abundance, although it does not affect the phenology of the life stages. Hence, we caution that the predicted abundance of *L. botrana* life stages can only be viewed as a metric of overall favourability of weather at each lattice location. A similar composite model was used with good success in predicting the geographical range and relative abundance of the exotic light brown apple moth *Epiphyas postvittana* in California that is attacked by a suite of native generalist natural enemies (Gutierrez *et al.*, 2010).

All sources of intrinsic and extrinsic mortality are combined and enter the dynamics model as a net proportional age-specific loss rate (i.e. μ_i in Eqn (A1)).

Diapause. Deseö *et al.* (1981) reported that *L. botrana* has a facultative autumn-hibernal type I diapause that with decreasing short-day photoperiods (dl) during autumn increasingly induces egg and early larval stages to become diapause pupae (Tzanakakis *et al.*, 1988). In the model, eggs and larvae destined
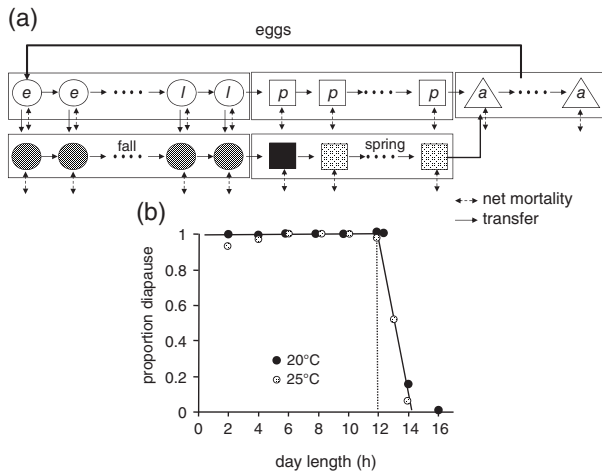
(a)

(b)

Figure 3 Submodel for diapause induction. (a) Age-structured models for the dynamics of nondiapause (open symbols) and diapause (dark stippled symbols) egg (*e*), larval (*l*), pupal (*p*) and adult (*a*) stages with flow from nondiapause age classes to same age diapause classes. Development of diapause eggs and larvae continue until they become first stage diapause pupae (black square) that, in spring, begin development (light stippled squares) to emerge as adults (for further explanation, see text). (b) The proportion of the eggs-larvae that will enter diapause on day length when reared at 20 or 25 °C (data from Roditakis & Karandinos, 2001).

to become diapause pupae flow (Fig. 3a, solid arrows) from non-diapause cohorts (Fig. 3a, open circles) to the same age diapause cohorts (Fig. 3a, closed stippled circles) where they continue development to pupation (Fig. 3a, black square). Diapause pupae remain quiescent until increasing temperatures during late winter and spring stimulate post-diapause development (Fig. 3a, stippled square) leading to adult emergence (Fig. 3a, bent upturned arrow) and oviposition. During autumn, larvae not entering diapause continue normal development to the adult stage and oviposition if hosts are available. After a short pre-oviposition period, newly emerged adult females from all sources deposit eggs that enter the first age class of the egg stage. The dashed double arrows indicate the net age-specific mortality rate (μ_i) in substage (*i*) as a result of all causes.

Two biodemographic models for diapause induction in *L. botrana* are available. The first is based on laboratory studies by Roditakis and Karandinos (2001) who exposed eggs and larvae to several diel and nondiel photoperiods at 20 and 25 °C and found that diapause is increasingly induced at day length (*dl*) below 14.15 h at both temperatures (Fig. 3b). Collapsing the data across the two temperatures yields Eqn (6i) ($0 \leq diap(dl) \leq 1$):

$$diap(dl) = \begin{cases} 0 \ for \ dl > 14.15h \\ \\ 0.4565 \times (14.15 - dl) \leq 1 \ for \ dl \leq 14.15h \end{cases}$$

(6i)

The second model is based on the observation by Riedl (1983) in codling moth of a north–south gradient for diapause induction, which Baumgärtner *et al.* (2012) explored for *L. botrana* using field data from across several locations across Europe. They

found that *dl* and latitude (*lat*) affected the diapause induction rates (*diap*(*dl*, *lat*)) (Eqn (6ii)):

$$0 \leq diap(dl, lat) = 4.487 + 0.056lat - 0.4565dl \leq 1, \quad (6ii)$$

Diapause models 6i and 6ii give qualitatively similar results (see Supporting Information, File S1) but, because of uncertainty in the field data and in fitting model Eqn (6ii), we use the simpler model (Eqn (6i)). The daily rate of diapause induction in eggs and young larvae ($\Delta diap_{e-1}(dl, T)$) is:

$$0 \leq \Delta diap(dl, T)_{e-1} = diap(dl) \cdot \frac{\Delta x_{e-1}}{\Delta_{e-1}} \leq 1, \quad (6iii)$$

where Δx_{e-1} is the change in age in degree days at temperature *T* at time *t*, and Δ_{e-1} is the egg-larval developmental time in $dd_{>8.9°C}$ on mature berries.

Emergence from diapause. The phenology and population dynamics of *L. botrana* vary with weather across locations and years. As temperatures rise above 11.5 °C in late winter and spring, diapause pupae begin development, yielding the first generation of new adults. Assuming a normal distribution, 95% of the diapausing pupae would be expected to emerge in 2 SDs from the mean. If the average developmental time of diapause pupae is $\Delta_{diap} = 115dd_{>11.5°C}$, then, from the definition of Erlang parameter $k = \Delta_{diap}^2/var$ in our distributed maturation time dynamics model, and assuming a conservative value of $k = 25$ and the $std = \sqrt{var} = 23dd_{>11.5°C}$ (see Appendix), the 2 SD window for emergence is $69dd_{>11.5°C}$ to $161.2dd_{>11.5°C}$. This approach worked well for modelling field data collected in the Napa Valley of California (Gutierrez *et al.*, 2012) and it is used here.

Weather data

Ambient daily weather data (maximum and minimum temperature, rainfall and solar radiation (MJ/m²/day) from the AgMERRA global weather dataset for the period 1 January 1980 to 31 December 2010 for 17 854 lattice cells (of approximately 25 × 25 km) for Europe and the Mediterranean Basin were used. Because of computational constraints (approximately 24–30 h per run on a laptop copmputer), only alternate lattice cells (i.e. 4506) were used to run the PBDMs. This coarser grain analysis does not affect the patterns or conclusions and is closer to the original spatial resolution of the underlying temperature data used to assemble the AgMERRA data set (Ruane *et al.*, 2015). The AgMERRA data are a daily time series of maximim−minimum temperatures, solar radiation, rainfall and relative humidity at an approximately 25-km geographical resolution for the period 1980–2010 (National Aeronautics & Space Administration, 2015; NASA). It was created as a baseline forcing dataset for the Agricultural Model Inter-comparison and Improvement Project (AgMIP; http://www.agmip.org/; Ruane *et al.*, 2015). This dataset was produced by combining a state-of-the-art reanalysis of weather observations (Modern-Era Retrospective analysis for Research and Applications, MERRA; Rienecker *et al.*, 2011) with observational datasets from
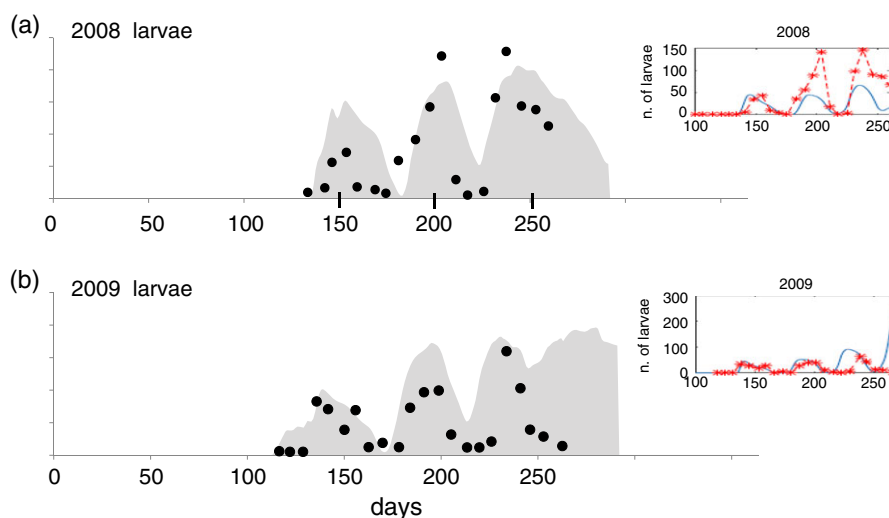
Figure 4 Scaled simulation of *Lobesia botrana* larval densities (grey) compared with field data (•) from Colognola ai Colli (Veneto region, Italy) for the (a) 2008 and (b) 2009 seasons (redrawn with persmission from Gilioli *et al*., 2016). Inset: data (x) and simulation (blue line) from Gilioli *et al*., 2016. [Colour figure can be viewed at wileyonlinelibrary.com].

in situ observational networks and satellites (Ruane *et al*., 2015). The AgMERRA data are used as the observed weather for the recent past.

The effects of projected climate warming on grapevine and *L. botrana* across the Palearctic region were examined by comparing climate model projections of the changes from a base period of 1960–1970 with a future 2040–2050 period (i.e. a climate change scenario). In the present study, we used the A1B regional climate change scenario that posits +1.8 °C warming for the Euro-Mediterranean region (Dell'Aquila *et al*., 2012). The A1B scenario is towards the middle of the IPCC (2014) range of greenhouse gas (GHG) forcing scenarios (Giorgi & Bi, 2005). The uncertainty associated with climate model predictions forced using the A1B scenario is low for the Mediterranean region relative to the rest of the globe (Gualdi *et al*., 2013). This fine scale weather dataset at an approximately 30-km resolution was developed by Dell'Aquila *et al*., 2012 using the regional climate model PROTHEUS (Artale *et al*., 2010) to refine and rescale the coarser (approximately 200-km resolution) global climate simulation forced with observed GHG for years 1951–2000 and the IPCC (2014) A1B GHG emissions scenario for 2001–2050. PROTHEUS is a coupled atmosphere–ocean regional model that allows simulation of local extremes of weather via the inclusion of a fine scale representation of topography and the influence of the Mediterranean Sea (Artale *et al*., 2010). The PROTHEUS A1B scenario is a finer scale projection of future climate change for the Euro-Mediterranean region and was used to run the grapevine/*L. botrana* system across the Palearctic region for the periods 1960–1970 and 2040–2050.

Data, simulation and GIS analysis

Batch files were used to initialize and run the model across all locations for the period of available weather data. The different species in Fig. 1 can be included in any run of the model using true-false Boolean variables from a batch file. The starting day for all runs was 1 January of the first year with an initial density

of four diapause pupae plant^{-1} (area = 2.3 m^2) assumed at all locations. Although the model predicts the density of grapevine subunits and all stages of *L. botrana*, we used the average annual yield per vine and the annual sum of *L. botrana* pupae per vine per year as the metrics of favourability for grape and of *L. botrana* infestation levels, respectively. The simulation data on a per vine basis were georeferenced and written to batch files by year for mapping and analysis. Because the model must equilibrate to the effects of local weather from the common initial conditions, the results for all simulation runs in the first year were not used to compute lattice cell averages, SDs and coefficient of variations as a percentage (CV).

The open source GIS GRASS originally developed by the United State Army Corp of Engineers was used to map the data using bicubic spline interpolation on a 3-km raster grid. The version of GRASS used is maintained and further developed by the GRASS Development Team (2014) (http://grass.osgeo.org).

Results

Figure 4 compares the scaled model predictions and field dynamics data for *L. botrana* larvae reported by Gilioli *et al*. (2016; inset figures) from Colognola ai Colli (Veneto Region, Italy) during 2008 and 2009 for days 100–265. Weather data from the nearest AgMERRA cell to Colognola ai Colli were used in the simulation. The goal was to gauge how well the model captured the phenology of *L. botrana* and not to make precise predictions of densities that are affected by net immigration from other hosts, grape cultivar, daily weather, predation, sampling error, etc. (see Supporting information, File S1). Larvae were detected earlier in 2009 than in 2008 with the largest discrepancies between the field data (•) and the simulation (the shaded area) in the present study (see Fig. 4) and in Gilioli *et al*. (2016) occurring during late season beyond the last field sampling date of day 265. Harvest dates vary between years and for different varieties and, in the model, occur at approximately 1850–1900$dd_{>10°C}$ (e.g. ~day 290). Note
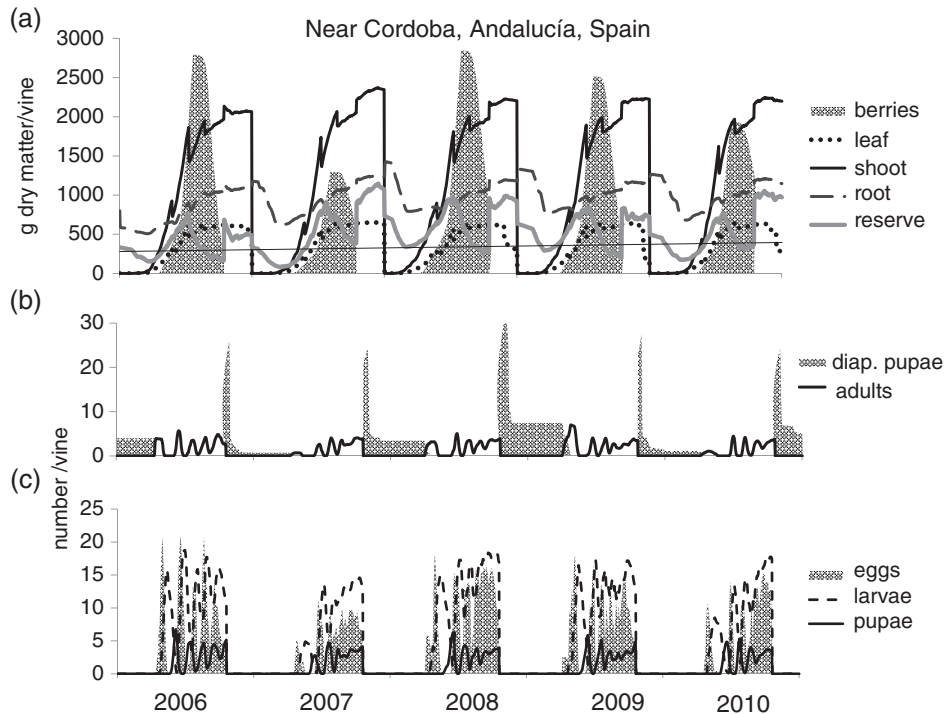
Figure 5 Simulation of the grapevine system dynamics near Cordoba (Andalucía region, Spain) (longitude −4.375, latitude 37.875) during 2006–2010. (a) Phenology of grapevine dry matter allocation dynamics, (b) dynamics of adult *Lobesia botrana* diapause pupae and adult dynamics and (c) the dynamics of egg production, larvae and nondiapause pupae.

that decreasing adult longevity 25% tightens the fit considerably (see Supporting information, File S1).

Simulated grapevine and L. botrana *dynamics near Cordoba (Andalucía region, Spain)*

For heuristic purposes, we use 2001–2010 weather data from a lattice cell near Cordoba (Andalucía region, Spain) (longitude −4.375, latitude 37.875) to illustrate the richness of the model output computed for all 4506 lattice cells. The full dynamics of the plant subunit population growth are shown in Fig. 5(a) (Wermelinger *et al*., 1991), whereas the dynamics of *L. botrana* life stages are illustrated in Fig. 5(b, c). The adult dynamics in Fig. 5(b) show the number of overwintering pupae (dark area) and the cumulative emergence of adult males and females. Figure 5(c) depicts the pattern of oviposition by reproductive adults of the different generations (Fig. 5c, shaded area) and the larval and pupal dynamics.

Adult generations per year

In Europe, more generations occur in hotter areas (e.g. Spain) (Martin-Vertedor *et al*., 2010) than in cooler areas. We demonstrate this by simulating adult dynamics at six locations in Spain along the −4.375° longitude at different latitudes during 1990–2010 (Fig. 6). The first peak each year is the emergence of adults in spring and the subsequent ones are summer generations. The number of generations at each location varies between

years as a result of weather conditions, with the relative number of generations given as appropriate. The fewest generations (two to three) are predicted for the mountainous areas of Cantabria in Northern Spain and increase to four to five generations in the northern parts of Andalucía near Cordoba.

A regional analysis of Europe and the Mediterranean Basin

System dynamics using observed 1980–2010 weather data. Figure 7(a,d) shows the prospective distribution of average annual grapevine yield and average *L. botrana* pupal density during the period 1980–2010 in the area of known grape production in the Palearctic region estimated from Monfreda *et al*. (2008) (see Supporting information, File S1). Highest yields occur in a broad band around 40°N latitude extending from Spain–Portugal in the west to Turkey in the east. The frequency distribution of average yield (Fig. 7b) shows a relative range 0–3500 g dry matter per plant. The CV as a percentage (Fig. 7c) also increases northward in response to colder more variable seasons and southward as a result of increasing high temperatures that affect yield. A high average yield and a low coefficient of variation for annual yield at each location characterize the region of highest favourability for grapevine.

Total annual pupal density and low CV are also metrics of climatic favourability for *L. botrana* at each location. Highest average density and low CV are predicted throughout the major regions of grape production (Fig. 7d–f). The highest CVs are predicted in Egypt and in colder northern areas.
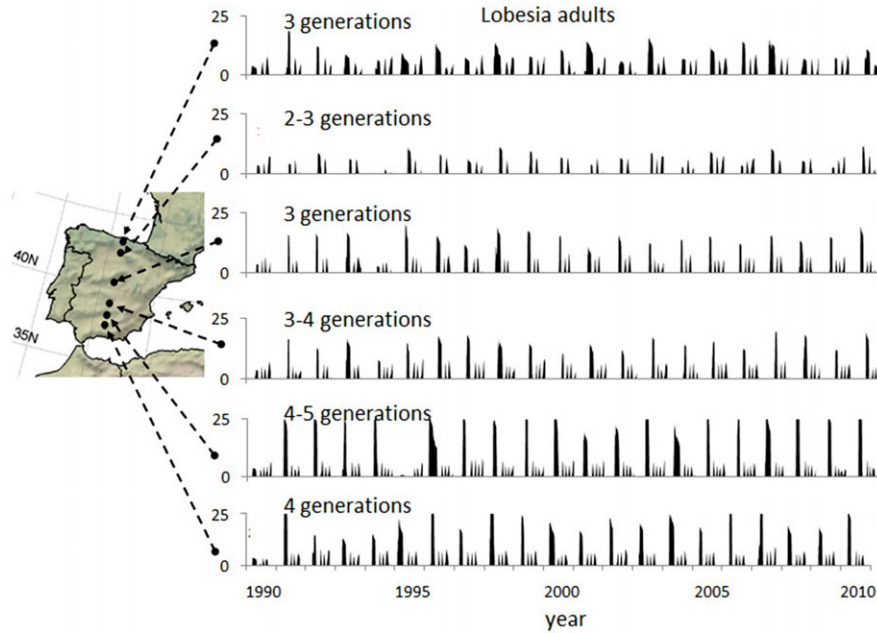
Figure 6 Simulated adult *Lobesia botrana* dynamics at six locations in Spain along the −4.375° longitude at different latitudes during years 1990−2010. The first dark peak in each year is the spring generation.[Colour figure can be viewed at wileyonlinelibrary.com].
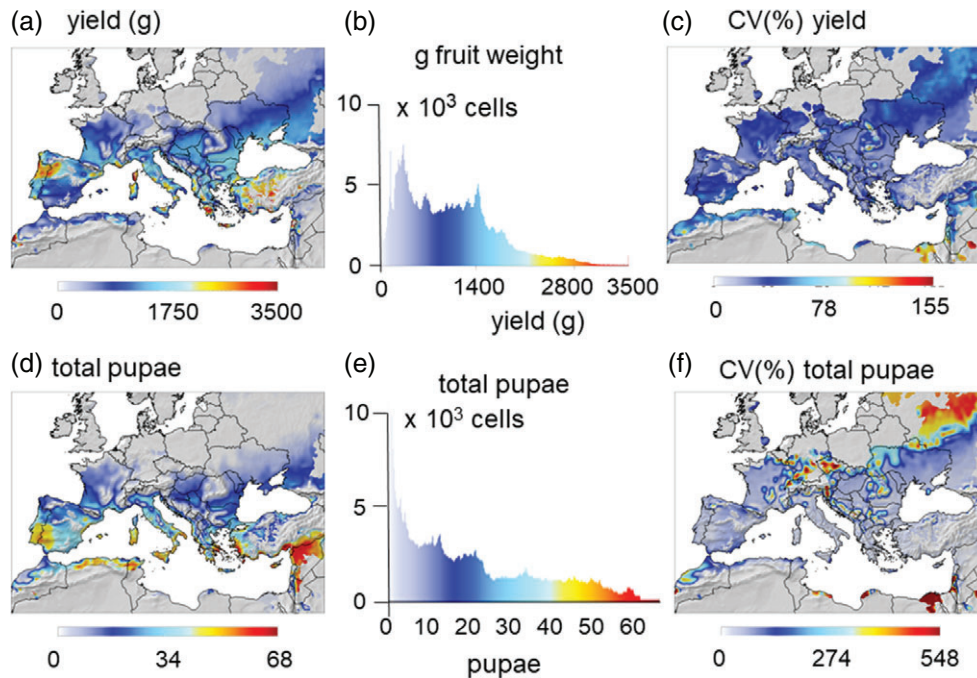

Figure 7 Prospective simulation of the grapevine/*Lobesia* system in the Palearctic region below 1500 m a.s.l during 1980−2010. (a) The distribution of average grape yield. (b) Frequency distribution of the number of lattice cells with different yield. (c) Coefficient of variation of yield as a percentage. (d) Distribution and abundance of *Lobesia botrana* pupal density. (e) Frequency histogram of cells with different pupal densities. (f) Coefficient of variation of pupal density as a percentage.
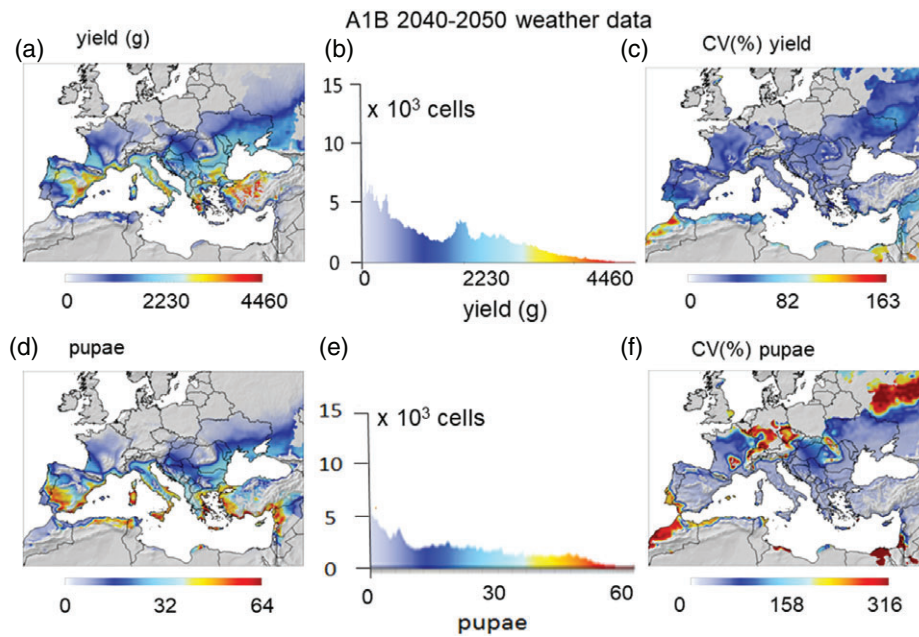
Figure 8 Prospective simulation of the grapevine/*Lobesia* system in the Palearctic region below 1500 m a.s.l. assuming a 1.8 °C increase in temperature during 2040−2050 (scenario A1B). (a) The distribution of average grape yield. (b) Histogram of the number of lattice cell with different yield. (c) Coefficient of variation of yield as a percentage. (d) Distribution and abundance of *Lobesia* pupal density. (e) Histogram of cell with different pupal densities. (f) Coefficient of variation of pupal density as a percentage.

System dynamics with +1.8 °C climate warming (A1B scenario). The yields under projected +1.8°C climate warming during 2040−2050 (IPCC, 2014, A1B GHG scenario) in the current Palearctic area of grapevine distribution are illustrated in Fig. 8(a). Regression of annual $dd_{>10\,°C}$ under the A1B scenario on those for the 1960−1970 baseline period shows a cumulative increase in physiological time of approximately 18.5% $[dd_{>10C,\,A1B} = 1.185 dd_{>10C,\,base}, R^2 = 0.993]$.

The effects of climate warming can be viewed by comparing average yields during the 2040−2050 period and the 1980−2010 period yields (Fig. 8a versus Fig. 7a). Specifically, average yield in currently favourable areas increases by approximately 10% as a result of climate warming; the range of favourability expands into more northern areas and higher elevations; the favourable geographical range declines with increasing CV in warmer North Africa and the Middle East (Fig. 8c versus Fig. 7c). Similarly, *L. botrana* pupal densities increase with climate warming in the areas favourable for grapevine, especially in areas of Spain, Greece and Turkey, but decline in areas of the Middle East (Fig. 8d versus Fig. 7d).

The effects of climate warming on the system dynamics across the region are best seen by plotting the difference between yields and pupal densities predicted using the IPCC A1B GHG scenario for 2040−2050 and those predicted for the baseline period 1960−1970 (Fig. 9a,c). Roughly, the largest increases in yield with climate warming are predicted in higher latitudes and elevations of Spain, Italy, southern France and in Turkey in the band around 40°N latitude and, to a lesser extent, northward in Europe where conditions for grapevine improve. Yields are unchanged or lower in areas of the Middle East and parts of North Africa. Plots of yields under the A1B scenario on the

base years 1960−1970 do not give a meaningful relationship (see Supporting information, File S1). However, using the same colour schema as in Fig. 9(a), the frequency distribution of changes in yield (Fig. 9b) shows a comparatively larger area with increased yield across the region than with yield declines.

Increases in *L. botrana* pupal abundance occur throughout a wide part of the region because warmer temperatures allow additional generations of the moth to develop (Fig. 9c). This change is best visualized by the frequency histogram of predicted change (i.e. Δpupae in Fig. 9d). A plot of Δyield on Δpupae (Fig. 9e) shows that *L. botrana* pupal densities not only increase in areas favourable for yield increases (+, +), but also in areas of yield decrease (−, +) (upper half quadrants). Pupal abundance may decrease in areas where yields decrease (lower left quadrant; −, −), although abundance never decrease in areas with yield increases (lower right quadrant; +, −).

Discussion

Grape is a mainstay cultural, economic and ecological factor of Mediterranean Basin and is the fruit crop with the largest acreage and the highest economic importance globally (Vivier & Pretorius, 2002). Grape and its pests have been the subject of considerable research efforts. Controlling infestation levels of the polyphagous grapevine moth has a high priority and several models have been developed for use in IPM decision support (Baumgärtner & Baronio, 1988; Briolini *et al.*, 1997; Schmidt *et al.*, 2003; Severini *et al.*, 2005; Gilioli *et al.*, 2016; Lanzarone *et al.*, 2017). In the present study, we used a weather-driven PBDM for grape vine and *L. botrana* that was developed based on European data and initially used to assess the invasiveness
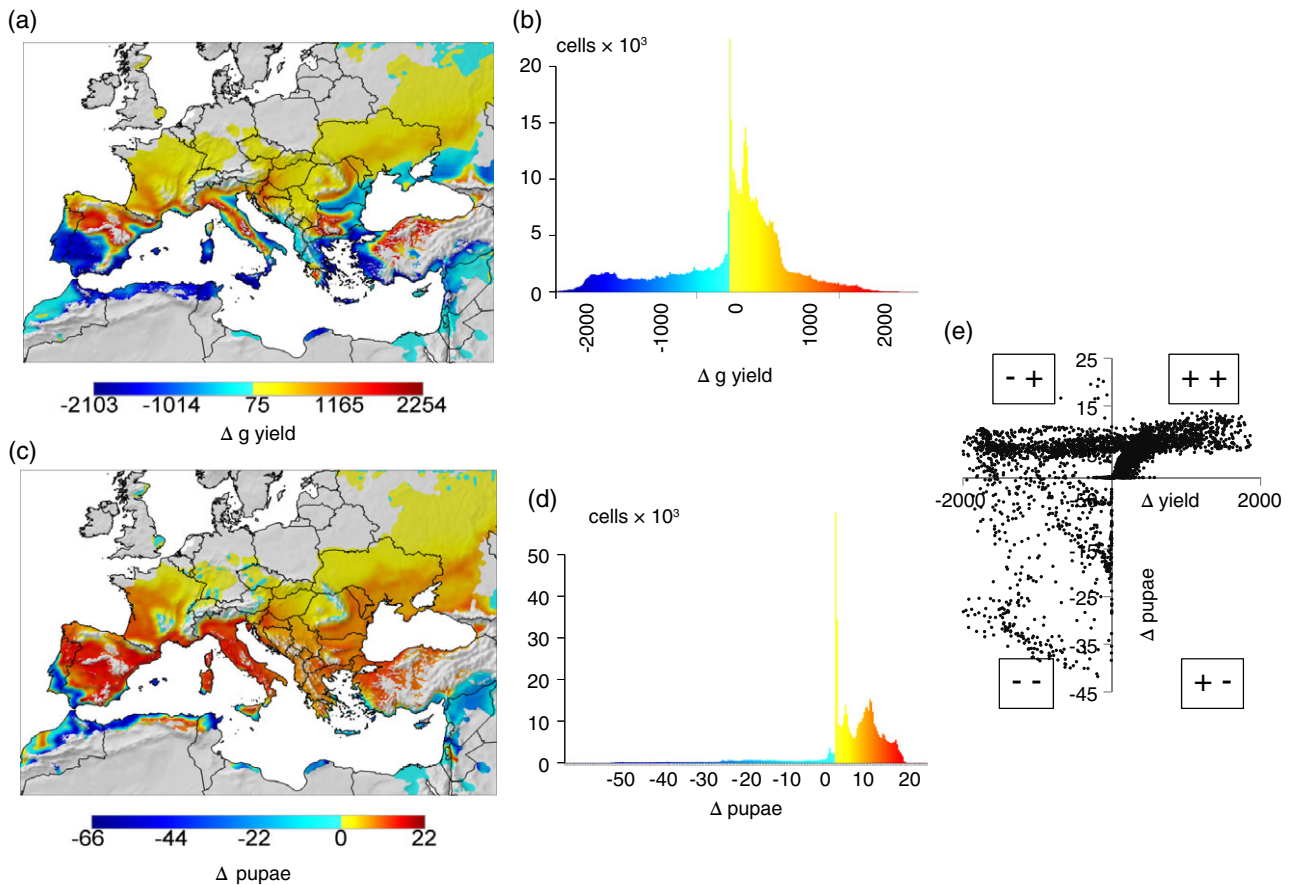
Figure 9 Comparison of prospective changes in the grapevine/*Lobesia* system in the Palearctic region below 1500 m a.s.l. given an A1B scenario of 1.8 °C average temperature increase between 2041–2050 (future) and 1960–1970 (baseline) simulated weather data. (a) The distribution of average changes in grape yield. (b) Histogram of the number of lattice cells with different levels of yield changes. (c) The distribution of average changes in the abundance of *Lobesia botrana* pupal density. (d) Histogram of cells with different levels of changes in pupal densities. (e) Plot of changes in yield (Δyield) on changes in pupal density (Δpupae).

and potential distribution and relative abundance of *L. botrana* in California after its accidental introduction in 2009 (Gutierrez *et al*., 2012). Because the PBDM is mechanistic and weather driven, it may be applied to any regions where grape is grown. The model was used to examine the favourability of observed weather for grape and *L. botrana* across the grape growing regions of the Palearctic, as well as to examine how favourability would change in the face of climate warming.

PBDMs are perceived to be difficult to develop, although this is not the case given an understanding of the biology and the simple mathematics of the population dynamics models and the availability of sound biological data (Gutierrez & Ponti, 2013). PBDMs may be viewed as time-varying life tables (*sensu* Gilbert *et al*., 1976). Multitrophic systems that include the bottom up dynamics of host plants on herbivore species and the top-down effects of higher trophic levels, as well as aspects of physiology and behavior, can be developed (Fig. 1). PBDM modelling of this level of complexity is facilitated by the fact that the same dynamics model are used for all species and the same forms for the biodynamic models reoccur for analogous processes in the life histories of all species across trophic levels (Gutierrez & Baumgärtner, 1984; Gutierrez *et al*., 2011; Gutierrez & Ponti,

2013). The development of PBDMs is facilitated by their modular structure enabling different combinations of species to be implemented in model runs using simple true-false Boolean variables, allowing the system to be viewed from the perspective of any of the interacting species (Gutierrez & Baumgärtner, 1984; Gutierrez & Ponti, 2013). The inclusion of rich biology allows prediction and mapping of the phenology, dynamics and relative abundance across a wide landscape with varied climates and future climate change. When the requisite biological data are not available, the model structure provides a useful guide for identifying the data gaps (Ponti *et al*., 2015) facilitating efficient gathering of the missing data to characterize the biodemographic functions and to make preliminary estimates of the pest dynamics. In the best case, PBDMs can be tested against field data (Rodríguez *et al*., 2013). The *PBDM* approach in a GIS context has been applied to many agroecological systems (Gutierrez *et al*., 2006, 2007, 2010, 2011, 2015, 2016; Ponti *et al*., 2014) and has provided considerable insights concerning the biology at the local and regional level useful in developing pest management practices and policy (see below). However, despite their considerable utility, we caution that all models including PBDMs are incomplete.

Regional dynamics of grape and L. botrana

In Europe, two distinct generations of *L. botrana* occur in Switzerland (Moraviea *et al.*, 2006), although three or even four may occur in southern Europe (Bovey, 1966; Gabel & Mocko, 1984; Milonas *et al.*, 2001; Roditakis & Karandinos, 2001). Martin-Vertedor *et al.* (2010) found four and a half generations in western Spain with a partial fifth recorded during 2006. A similar range of generations was predicted from seven locations on a north–south gradient in California (Gutierrez *et al.*, 2012) and on a north–south gradient in Spain in the present study (Fig. 6). Under nonlimiting water, the number of generations of *L. botrana* is determined largely by temperature and photoperiod and the availability of hosts. Studies on the spatial distribution of *L. botrana* in central Italy showed that its distribution among hosts is not limited to vineyards because a high presence may occur in olive groves and in other hosts not normally considered in grape pest management practices (Sciarretta *et al.*, 2008).

Climate warming effects. Climate warming (and increased CO_2 levels) will likely not only affect development of the grapevine and yield, but also higher trophic levels (Caffarra *et al.*, 2012; Reineke & Thiéry, 2016). Because PBDMs are driven by weather, their application is not time and place specific, and they can readily be extended to examine the effects of climate change scenarios, or historical observations such as those of Martin-Vertedor *et al.* (2010), who found evidence that climate warming during 1984–2006 in six vine-growing areas of western Spain caused earliness of adult flights of more than 12 days and increased voltinism.

To examine the effects of climate warming, we used weather data from a fine-scale regional climate model simulation (Artale *et al.*, 2010; Dell'Aquila *et al.*, 2012) based on the A1B scenario of intermediate climate change (IPCC, 2014) that predicts an average increase in daily temperatures of +1.8 °C for years 2040–2050 versus 1960–1970 across the Euro-Mediterranean region. The model predicts that grapevine yields will increase northward and in higher elevations, although they will decrease in more southern areas of the extant distribution as temperatures approach the upper thermal limits for grape (and where water becomes limiting). The relative abundance of *L. botrana* will increase generally throughout the grape growing region. In more northern areas, warmer temperatures will decrease winter mortality and increase the summer reproductive period (see Supporting information, File S1). By contrast, *L. botrana* levels may decrease in southern areas (e.g. southwestern Spain, Morocco) where high summer temperatures approach or exceed the upper thermal limits of the moth and adversely affect its vital rates (Fig. 9c). The apparent large changes in southwestern Spain and Morocco are artefacts of the insensitivity of the colour bar scale selected to illustrate the changes in the larger area of the Palearctic range of the moth. For this reason, the maps for the A1B 2040–2050 and 1961–1970 results are illustrated on a different scale in the Supporting information (File S1) and show that the increases and decreases in *L. botrana* in southwestern Spain and Morocco were mostly < 10 pupae. Similar declines in pupal densities are predicted for the Eastern Mediterranean region (Syria, Lebanon, Israel and Palestine).

In summary, *L. botrana* populations will increase as a result of climate change in most areas where grape yield increase, although levels may increase or decrease where grape yields decrease (Fig. 9e). Hence, control of *L. botrana* is essential, and sound PBDMs can be useful and for developing and evaluating control strategies locally and regionally, and implementing them in real time (Gilioli *et al.*, 2016).

Control of L. botrana

Many parasitoids and predators attack *L. botrana* immature stages (Scaramozzino *et al.*, 2017), although they do not provide economic control (Xuéreb & Thiéry, 2006; Bărbuceanu & Jenser, 2009) and hence ecologically sound IPM control strategies are required. The wide range of wild host plants in the Palearctic region (http://www.cabi.org/isc/datasheet/42794) complicates control. In Europe, insecticides and mating disrupting pheromones are commonly used for control of *L. botrana* (Oliva *et al.*, 1999; Ifoulis & Savopoulou-Soultani, 2004), although biopesticides such as *Bacillus thuringiensis* show promise (Ioriatti *et al.*, 2011; Pertot *et al.*, 2016).

The economic thresholds for insecticide control of *L. botrana* are qualitative, and depend on the moth generation, the susceptibility of the cultivar to infection by *Botrytis*, as well as whether the grapes are produced for table fruit or wine (Ioriatti *et al.*, 2008, 2011). The proper timing of conventional insecticides targeting adult flights is critical for effective control (Caffarelli & Vita, 1988; Oliva *et al.*, 1999; Boselli & Scannavini, 2001) and several phenological models have been developed to forecast the flight of the different generations of adult moths (Gabel & Mocko, 1984; Caffarelli & Vita, 1988; Del Tío *et al.*, 2001; Milonas *et al.*, 2001; Moraviea *et al.*, 2006; Gallardo *et al.*, 2009; Gutierrez *et al.*, 2012; Gilioli *et al.*, 2016).

In Europe, the use of pheromones for detection and control of *L. botrana* by mating disruption is well developed (Harari *et al.*, 2007) and, unlike pesticide use, precise timing is less critical as the period of pheromone efficacy is quite long, although coverage must be continuous during the season (Anfora *et al.*, 2008). Pheromones reduce the reproductive output of the population (Torres-Vila *et al.*, 2002), although effectiveness depends on temperature and wind speed, rate of pheromone release, size of the target area, cultural practices, the presence of alternate host plants that serve as unregulated sources of adult moths (Vassiliou, 2009) and the slope of the land (Carlos *et al.*, 2010). Effectiveness is inversely density-dependent and insecticide use may be required at high moth densities (Gordon *et al.*, 2005). Good control of *L. botrana* has been demonstrated in Europe using pheromone applied against the flight of spring generation adults, with additional pheromone dispensers being applied starting in early June against the first and later summer flights (Anfora *et al.*, 2008; Vassiliou, 2009; Ioriatti *et al.*, 2011). The pheromone strategy has been most effective when applied on an area wide basis (Ioriatti *et al.*, 2011). Simulation and marginal analysis using a PBDM for *L. botrana* in California predicted recommendations for mating disruption similar to those of the above field studies (see Supporting information, File S1) (Gutierrez *et al.*, 2012). Furthermore, under climate warming, the first generation flight of adults would occur earlier and the

season would be longer with one or more additional generations, although this would not alter the underpinning pheromone-based control strategy.

Last, at the strategic level, PBDMs can be used as the production function in a bio-economic analysis of grape to assess local and regional impact of different pests, disease and control strategies under extant and climate change scenarios (Regev *et al.*, 1998; Pemsl *et al.*, 2007; Ponti *et al.*, 2014; Gutierrez *et al.*, 2015).

Acknowledgements

Supporting information

Additional Supporting information may be found in the online version of this article under the DOI reference: 10.1111/afe.12256

File S1. Supporting information for the effects of climate warming on grape and grapevine moth.

References

Ainseba, B., Picart, D. & Thiéry, D. (2011) An innovative multistage, physiologically structured, population model to understand the European grapevine moth dynamics. *Journal of Mathematical Analysis and Applications*, **382**, 34–46.

Andreadis, S., Panagiotis, S., Milonas, G. & Savopoulou-Soultani, M. (2005) Cold hardiness of diapausing and non-diapausing pupae of the European grapevine moth, *Lobesia botrana*. *Entomologia Experimentalis et Applicata*, **117**, 113–118.

Anfora, G., Baldessari, M., De Cristofaro, A. *et al.* (2008) Control of *Lobesia botrana* (Lepidoptera: Tortricidae) by biodegradable ecodian sex pheromone dispensers. *Journal of Economic Entomology*, **101**, 444–450.

Artale, V., Calmanti, S., Carillo, A. *et al.* (2010) An atmosphere-ocean regional climate model for the Mediterranean area: assessment of a present climate simulation. *Climate Dynamics*, **35**, 721–740.

Bărbuceanu, D. & Jenser, G. (2009) The parasitoid complex of *Lobesia botrana* (Denis et Schiffermüller) (Lep.: Tortricidae) in some vineyards of southern Romania. *Acta Phytopathologica et Entomologica Hungarica*, **44**, 177–184.

Baumgärtner, J. & Baronio, P. (1988) Modello fenologico di volo di *Lobesia botrana* Den. et Schiff. (Lep. Tortricidae) relativo alla situazione ambientale della Emilia-Romagna. *Bollettino dell'Istituto di Entomologia della Università di Bologna 'Guido Grandi' dell'Università di Bologna*, **43**, 157–170.

Baumgärtner, J., Gutierrez, A.P., Pesolillo, S. & Severini, M. (2012) A model for the overwintering process of European grapevine moth (*Lobesia botrana*) populations. *Journal of Entomological and Acarological Research*, **44**, e2.

Bieri, M., Baumgärtner, J., Bianchi, G., Delucchi, V. & von Arx, R. (1983) Development and fecundity of pea aphid (*Acyrthosiphon pisum* Harris) as affected by constant temperatures and by pea varieties. *Mitteilungen der Schweizerischen Entomologischen Gesellschaft*, **56**, 163–171.

Boselli, M. & Scannavini, M. (2001) Lotta alla tignoletta della vite in Emilia Romagna. *Informatore Agrario*, **19**, 97–100.

Bovey, P. (1966) L'eudémis de la vigne. *Entomologie Appliqueé 'a L'Agriculture*, Tome II: Lépidoptères, Vol. **1**. pp. 859–887. Masson, France.

Brière, J.F. & Pracros, P.C. (1998) Comparison of temperature dependent growth models with the development of *Lobesia botrana* (Lepidoptera: Tortricidae). *Environmental Entomology*, **27**, 94–101.

Brière, J.F., Pracros, P.C., Le Roux, A.Y. & Pierre, S.J. (1999) A novel rate model of temperature-dependent development for arthropods. *Environmental Entomology.*, **28**, 22–29.

Briolini, G., Di Cola, G. & Gilioli, G. (1997) Stochastic model for population development of *Lobesia botrana* (Den. et Schiff.). *IOBC/WPRS Bulletin*, **21**, 79–81.

Buffoni, G. & Pasquali, S. (2007) Structured population dynamics: continuous size and discontinuous stage structures. *Journal of Mathematical Biology*, **54**, 555–595.

Caffarelli, V. & Vita, G. (1988) Heat accumulation for timing grapevine moth control measures. *Bulletin OILB-SROP*, **11**, 24–26.

Caffarra, A., Rinaldi, M., Eccel, E., Rossi, V. & Pertot, I. (2012) Modelling the impact of climate change on the interaction between grapevine and its pests and pathogens: European grapevine moth and powdery mildew. *Agriculture, Ecosystems & Environment*, **148**, 89–101.

Carlos, C., Alves, F. & Torres, L. (2010) Eight years of practical experience with mating disruption to control grape berry moth, *Lobesia botrana*, in Porto Wine Region. *Proceedings of the 7th International Conference on Integrated Fruit Production, 27–30 October 2008, Avignon, France* (eds by J. Cross, M. Brown, J. Fitzgerald, M. Fountain and D. Yohalem), pp. 405–409. IOBC/WPRS Bulletin, France.

Dell'Aquila, A., Calmanti, S., Ruti, P., Struglia, M.V., Pisacane, G., Carillo, A. & Sannino, G. (2012) Effects of seasonal cycle fluctuations in an A1B scenario over the Euro-Mediterranean region. *Climate Research*, **52**, 135–157.

Del Tío, R., Martinez, J.L. & Ocete, M.E. (2001) Study of the relationship between sex pheromone trap catches of *Lobesia botrana* (Den. and Schiff.) (Lep., Tortricidae) and the accumulation of degree-days in Sherry vineyards (SW of Spain). *Journal of Applied Entomology*, **125**, 9–14.

Deseő, K.V., Marani, F., Brunelli, A. & Bertaccini, A. (1981) Observations on the biology and diseases of *Lobesia botrana* Den. and Schiff. (Lepidoptera: Tortricidae) in Central-North Italy. *Acta Phytopathologica Academiae Scientiarum Hungaricae*, **1**, 405–431.

DiCola, G., Gilioli, G. & Baumgärtner, J. (1999) Mathematical models for age-structured population dynamics. *Ecological Entomology*, 2nd edn (ed. by C. B. Huffaker and A. P. Gutierrez), pp. 503–531. John Wiley & Sons, New York, New York.

Fermaud, M. & Giboulot, A. (1992) Influence of *Lobesia botrana* larvae on field severity of *Botrytis* rot on grape berries. *Plant Disease*, **76**, 404–409.

Gabel, B. (1981) Effect of temperature on the development and reproduction of the grape moth, *Lobesia botrana* (Den. & Schiff.) (Lepidoptera, Tortricidae). *Anzeiger für Schädlingskunde, Pflanzenschutz, Umweltschutz*, **54**, 83–87.

Gabel, B. & Mocko, V. (1984) Forecasting the cyclical timing of grapevine moth, *Lobesia botrana* (Lepidoptera, Tortricidae). *Acta Entomologica Bohemoslovaca*, **81**, 1–14.

Gabel, B. & Roehrich, R. (1995) Sensitivity of grapevine phenological stages to larvae of European grapevine moth, *Lobesia botrana* den et Schiff (Lep, Tortricidae). *Journal of Applied Entomology*, **119**, 127–130.

Gallardo, A., Ocetel, R., Lopez, M.A., Maistrello, L., Ortega, F., Semedo, A. & Soria, F.J. (2009) Forecasting the flight activity of *Lobesia botrana* (Denis and Schiffermüller) (Lepidoptera, Tortricidae) in southwestern Spain. *Journal of Applied Entomology*, **133**, 626–632.

Gilbert, N., Gutierrez, A.P., Frazer, B.D. & Jones, R.E. (1976) *Ecological Relationships*. W.H. Freeman & Company, U.K.

Gilioli, G., Pasquali, S. & Marchesini, E. (2016) A modelling framework for pest population dynamics and management: an application to the grape berry moth. *Ecological Modelling*, **320**, 348–357.

Giorgi, F. & Bi, X. (2005) Updated regional precipitation and temperature changes for the 21st century from ensembles of recent AOGCM simulations. *Geophysical Research Letters*, **32**, L21715.

Gordon, D., Zahavi, T., Anshelevich, L., Harel, M., Ovadia, S., Dunkelblum, E. & Harari, A.R. (2005) Mating disruption of *Lobesia botrana* (Lepidoptera: Tortricidae): effect of pheromone formulations and concentrations. *Journal of Economic Entomology*, **98**, 135–142.

González-Domínguez, E., Caffi, T., Ciliberti, N. & Rossi, R. (2015) A mechanistic model of *Botrytis cinerea* on grapevines that includes weather, vine growth stage, and the main infection pathways. *PLoS ONE*, **10**, e0140444.

GRASS Development Team (2014) *Geographic Resources Analysis Support System* (*GRASS*) *Software*, *Version 6.4.4*. Open Source Geospatial Foundation. [WWW document]. URL http://grass.osgeo.org [accessed on 12 August 2017].

Gualdi, S., Somot, S., Li, L. *et al.* (2013) The CIRCE simulations: regional climate change projections with realistic representation of the Mediterranean Sea. *Bulletin of the American Meteorological Society*, **94**, 65–81.

Gutierrez, A.P. (1992) Physiological basis of ratio-dependent predator-prey theory: the metabolic pool model as a paradigm. *Ecology*, **73**, 1529–1553.

Gutierrez, A.P. (1996) *Applied Population Ecology: A Supply-demand Approach*. John Wiley and Sons, Inc., New York, New York.

Gutierrez, A.P. & Baumgärtner, J. (1984) Multi-trophic level models of predator-prey energetics: II. A realistic model of plant-herbivore-parasitoid-predator interactions. *Canadian Entomologist*, **116**, 933–949.

Gutierrez, A.P., Daane, K.M., Ponti, L., Walton, V.M. & Ellis, C.K. (2007) Prospective evaluation of the biological control of the vine mealybug: refuge effects. *Journal of Applied Ecology*, **44**, 1–13.

Gutierrez, A.P., Mills, N.J. & Ponti, L. (2010) Limits to the potential distribution of light brown apple moth in Arizona-California based on climate suitability and host plant availability. *Biological Invasions*, **12**, 3319–3331.

Gutierrez, A.P. & Ponti, L. (2013) Eradication of invasive species: why the biology matters. *Environmental Entomology*, **42**, 395–411.

Gutierrez, A.P., Ponti, L., Cooper, M.L., Gilioli, G., Baumgärtner, J. & Duso, C. (2012) Prospective analysis of the invasive potential of the European grapevine moth *Lobesia botrana* (Den. & Schiff.) in California. *Agricultural and Forest Entomology*, **14**, 225–238.

Gutierrez, A.P., Ponti, L., Cristofaro, M., Smith, L. & Pitcairn, M.J. (2016) Assessing the biological control of yellow starthistle (*Centaurea solstitialis* L): prospective analysis of the impact of the rosette weevil (*Ceratapion basicorne* (Illiger)). *Agricultural and Forest Entomology*, **19**, 257–273.

Gutierrez, A.P., Ponti, L., Ellis, C.K. & d'Oultremont, T. (2006) *Analysis of Climate Effects on Agricultural Systems: A Report to the Governor of California Sponsored by the California Climate Change Center*. [WWW document]. URL http://www.energy.ca.gov/2005publications/CEC-500-2005-188/CEC-500-2005-188-SF.PDF [accessed on 12 August 2017].

Gutierrez, A.P., Ponti, L., Herren, H.R., Baumgärtner, J. & Kenmore, P.E. (2015) Deconstructing Indian cotton: weather, yields and suicides. *Environmental Sciences Europe*, **27**, 12 (17 p.). https://doi.org/10.1186/s12302-015-0043-8.

Gutierrez, A.P., Ponti, L., Hoddle, M., Almeida, R.P.P. & Irvin, N.A. (2011) Geographic distribution and relative abundance of the invasive glassy winged sharpshooter: effects of temperature and egg parasitoids. *Environmental Entomology*, **40**, 755–769.

Gutierrez, A.P., Williams, D.W. & Kido, H. (1985) A model of grape growth and development: the mathematical structure and biological considerations. *Crop Science*, **25**, 721–728.

Harari, A.R., Zahavi, T., Gordon, D., Anshelevich, L., Harel, M., Ovadia, S. & Dunkelblum, E. (2007) Pest management programmes in vineyards using male mating disruption. *Pest Management Science*, **63**, 769–775.

Heit, G., Sione, W. & Cortese, P. (2015) Three years analysis of *Lobesia botrana* (Lepidoptera: Tortricidae) flight activity in a quarantined area. *Journal of Crop Protection*, **4** (Suppl.), 605–615.

Ifoulis, A.A. & Savopoulou-Soultani, M. (2004) Biological control of *Lobesia botrana* (Lepidoptera: Tortricidae) larvae by using different formulations of *Bacillus thuringiensis* in 11 vine cultivars under field conditions. *Journal of Economic Entomolgy*, **97**, 340–343.

Ioriatti, C., Anfora, G., Tasin, M., Cristofaro, A.D., Witzgall, P. & Lucchi, A. (2011) Chemical ecology and management of *Lobesia botrana* (Lepidoptera: Tortricidae). *Journal of Economic Entomology*, **104**, 1125–1137.

Ioriatti, C., Lucchi, A. & Bagnoli, B. (2008) Grape area wide pest management in Italy. *Areawide Pest Management: Theory and Implementation* (ed. by O. Koul, G. W. Cuperus and N. Elliott), pp. 208–225. CABI International, U.K.

IPCC (2014) Reports 'Impacts, Adaptation and Vulnerability', Fourth and Fifth Assessment Reports of the Intergovernmental Panel on Climate Change. [WWW document]. URL http://ipcc-wg2.gov/publications/Reports/ [accessed on 12 August 2017].

Lanzarone, E., Pasquali, S., Gilioli, G. & Marchesini, E. (2017) A Bayesian estimation approach for the mortality in a stage-structure demographic model. *Journal of Mathematical Biology*, **75**, 759–779.

Maher, N. & Thiery, D. (2006) *Daphne gnidium*, a possible native host plant of the European grapevine moth *Lobesia botrana*, stimulates its oviposition. Is a host shift relevant? *Chemoecology*, **16**, 135–144.

Marchesini, E. & Dalla Montà, L. (1994) Observations on natural enemies of *Lobesia botrana* (den. & Schiff.) (Lepidoptera, Tortricidae) in Venetian vineyards. *Bollettino di Zoologia Agraria e di Bachicoltura Series II*, **26**, 201–230.

Manetsch, T.J. (1976) Time-varying distributed delays and their use in aggregate models of large systems. *IEEE Transactions on Systems Man and Cybernetics*, **6**, 547–553.

Manly, B.F.J. (1989) A review of methods for the analysis of stage-frequency data. *Estimation and Analysis of Insect Populations* (ed. by L. McDonald, B. Manly, J. Lockwood and J. Logan), pp. 3–69. Springer, Germany.

Martin-Vertedor, D., Ferrero-Garcia, J.J. & Torres-Vila, L.M. (2010) Global warming affects phenology and voltinism of *Lobesia botrana* in Spain. *Agricultural and Forest Entomology*, **12**, 169–176.

Milonas, P.G., Savopoulou-Soultani, M. & Stavridis, D.G. (2001) Day-degree models for predicting the generation time and flight activity of local populations of *Lobesia botrana* (Den. and Schiff.)

(Lep., Tortricidae) in Greece. *Journal of Applied Entomology*, **125**, 515–518.

Monfreda, C., Ramankutty, N. & Foley, J.A. (2008) Farming the planet: 2. Geographic distribution of crop areas, yields, physiological types, and net primary production in the year 2000. *Global Biogeochemical Cycles*, **22**, GB1022.

Moraviea, M.A., Davisona, A.C., Pasquier, D. & Charmillot, P.J. (2006) Bayesian forecasting of grape moth emergence. *Ecological Modelling*, **197**, 478–489.

Moreau, J., Monceau, K. & Thiéry, D. (2016) Larval food influences temporal oviposition and egg quality traits in females of *Lobesia botrana*. *Journal of Pest Science*, **89**, 439–448.

NASA (National Aeronautics and Space Administration) (2015) AgMERRA and AgCFSR Climate Forcing Datasets for Agricultural Modeling. Goddard Institute for Space Studies. http://data.giss.nasa.gov/impacts/agmipcf/.

Nicholson, A.J. & Bailey, V.A. (1935) The balance of animal populations. Part1. *Proceeding of the Zoological Society of London*, **3**, 551–598.

Oliva, J., Navarro, S., Navarro, G., Camara, M.A. & Barba, A. (1999) Integrated control of grape berry moth (*Lobesia botrana*), powdery mildew (*Uncinula necator*), downy mildew (*Plasmopara viticola*) and grapevine sour rot (*Acetobacter spp.*). *Crop Protection*, **18**, 581–587.

Pemsl, D., Gutierrez, A.P. & Waibel, H. (2007) The economics of biotechnology under ecosystems disruption. *Ecological Economics*, **66**, 177–183.

Pertot, I., Caffi, T., Rossi, V. *et al.* (2016) A critical review of plant protection tools for reducing pesticide use on grapevine and new perspectives for the implementation of IPM in viticulture. *Crop Protection*, **97**, 70–84.

Ponti, L., Gilioli, G., Biondi, A., Desneux, N. & Gutierrez, A.P. (2015) Physiologically based demographic models streamline identification and collection of data in evidence-based pest risk assessment. *EPPO Bulletin*, **45**, 317–322.

Ponti, L., Gutierrez, A.P., Ruti, P.M. & Dell'Aquila, A. (2014) Fine-scale ecological and economic assessment of climate change on olive in the Mediterranean Basin reveals winners and losers. *Proceedings of the National Academy of Sciences, USA*, **111**, 5598–5603.

Potter, K.A., Woods, H.A. & Pincebourde, S. (2013) Microclimatic challenges in global change biology. *Global Change Biology*, **19**, 2932–2939.

Regev, U., Gutierrez, A.P., Schreiber, S.J. & Zilberman, D. (1998) Biological and economic foundations of renewable resource exploitation. *Ecological Economics*, **26**, 227–242.

Reineke, A. & Thiéry, D. (2016) Grapevine insect pests and their natural enemies in the age of global warming. *Journal of Pest Science*, **89**, 313–328.

Riedl, H. (1983) Analysis of codling moth phenology in relation to latitude, climate and food availability. *Diapause and Life Cycle Strategies in Insects* (ed. by V. K. Brown and I. Hodek), pp. 233–253. Dr W. Junk Publishers, The Netherlands.

Rienecker, M.M., Suarez, M.J., Gelaro, R. *et al.* (2011) MERRA: NASA's modern-era retrospective analysis for research and applications. *Journal of Climate*, **24**, 3624–3648.

Roditakis, N. & Karandinos, M. (2001) Effects of photoperiod and temperature on pupal diapause induction of grape berry moth *Lobesia botrana*. *Physiological Entomology*, **26**, 329–340.

Rodríguez, D., Cure, J.R., Gutierrez, A.P., Cotes, J.M. & Cantor, F. (2013) A coffee agroecosystem model: II. Dynamics of coffee berry borer. *Ecological Modelling*, **248**, 203–214.

Ruane, A.C., Goldberg, R. & Chryssanthacopoulos, J. (2015) Climate forcing datasets for agricultural modeling: merged products for gap-filling and historical climate series estimation. *Agricultural and Forest Meteorology*, **200**, 233–248.

Savopoulou-Soultani, M. & Tzanakakis, M.E. (1988) Development of *Lobesia botrana* (Lepidoptera, Tortricidae) on grapes and apples infected with the fungus *Botrytis cinerea*. *Environmental Entomology*, **17**, 1–6.

Savopoulou-Soultani, M., Stavridis, D.G. & Tzanakakis, M.E. (1990) Development and reproduction on *Lobesia botrana* on grapevine and olive inflorescences. *Entomologica Hellenica*, **8**, 29–35.

Savopoulou-Soultani, M., Milonas, P.G. & Skoulakis, G.E. (1996) Development and life-fertility tables for *Lobesia botrana* (Lepidoptera: Tortricidae) at constant temperatures. *Recent Research Developments in Entomology*, **1**, 73–81.

Savopoulou-Soultani, M., Nikolaou, N. & Milonas, G.P. (1999) Influence of maturity stage of the grape berries on the development of *Lobesia botrana* (Lepidoptera: Tortricidae) larvae. *Journal of Economic Entomology*, **92**, 551–556.

Scaramozzino, P.L., Loni, A. & Lucchi, A. (2017) A review of insect parasitoids associated with *Lobesia botrana* (Denis & Schiffermüller, 1775) in Italy. 1. Diptera Tachinidae and Hymenoptera Braconidae (Lepidoptera: Tortricidae). *ZooKeys*, **647**, 67–100.

Schmidt, K., Hoppmann, D., Holst, H. & Berkelmann-Löhnertz, B. (2003) Identifying weather-related covariates controlling grape berry moth dynamics. *OEPP/EPPO Bulletin*, **33**, 517–524.

Sciarretta, A., Zinni, A., Mazzocchetti, A. & Trematerra, P. (2008) Spatial analysis of *Lobesia botrana* (Lepidoptera: Tortricidae) male population in a Mediterranean agricultural landscape in central Italy. *Environmental Entomology*, **37**, 382–390.

Severini, M., Alilla, R., Pesolillo, S. & Baumgärtner, J. (2005) Fenologia della vite e della *Lobesia botrana* (Lep. Tortricidae) nella zona dei Castelli Romani. *Rivista Italiana di Agrometeorologia*, pp. 34–39.

Thiéry, D. & Moreau, J. (2005) Relative performance of European grapevine moth (*Lobesia botrana*) on grapes and other hosts. *Oecologia*, **143**, 548–557.

Thiéry, D., Monceau, K. & Moreau, J. (2014) Different emergence phenology of European grapevine moth (Lobesia botrana, Lepidoptera: Tortricidae) on six varieties of grapes. *Bulletin of Entomological Research*, **104**, 277–287.

Torres-Vila, L.M., Stockel, J., Roehrich, R. & Rodríguez-Molina, M.C. (1997) The relation between dispersal and survival of *Lobesia botrana* larvae and their density in vine inflorescences. *Entomologia Experimentalis et Applicata*, **84**, 109–114.

Torres-Vila, L.M., Rodriguez-Molina, M.C., Roehrich, R. & Stockel, J. (1999) Vine phenological stage during larval feeding affects male and female reproductive output of *Lobesia botrana* (Lepidoptera: Tortricidae). *Bulletin of Entomological Research*, **89**, 549–556.

Torres-Vila, L.M., Rodriguez-Molina, M.C. & Stockel, J. (2002) Delayed mating reduces reproductive output of female European grapevine moth, *Lobesia botrana* (Lepidoptera: Tortricidae). *Bulletin of Entomological Research*, **92**, 241–249.

Tzanakakis, M.E., Savopoulou-Soultani, M., Oustapassidis, C.S., Verras, S.C. & Hatziemmanuel, H. (1988) Induction of dormancy in *Lobesia botrana* by long day and high temperature conditions. *Entomologica Hellenica*, **6**, 7–10.

Vansickle, J. (1977) Attrition in distributed delay models. *IEEE Transactions on Systems Man and Cybernetics*, **7**, 635–638.

Varela, L.G., Smith, R.J., Cooper, M.L. & Hoenisch, R.W. (2010) European Grapevine Moth, *Lobesia botrana*, in Napa Valley Vineyards. *Practical Winery and Vineyard*, 1–5.

Vassiliou, V.A. (2009) Control of *Lobesia botrana* (Lepidoptera: Tortricidae) in vineyards in Cyprus using the mating disruption technique. *Crop Protection*, **28**, 145–150.

Venette, R.C., Davis, E.E., Da Costa, M., Heisler, H. & Larson, M. (2003) *Mini Risk Assessment – Grape Berry Moth*, Lobesia botrana (*Denis and Schiffermüller*) *[Lepidoptera: Tortricidae]*. USDA CAPS PRA, 29 pp.

Vivier, M.A. & Pretorius, I.S. (2002) Genetically tailored grapevines for the wine industry. *Trends in Biotechnology*, **20**, 472–478.

Wermelinger, B., Baumgärtner, J. & Gutierrez, A.P. (1991) A demographic model of assimilation and allocation of carbon and nitrogen in grapevines. *Ecological Modelling*, **53**, 1–26.

Winkler, A.J., Cook, J.A., Kliewer, W.M. & Lider, L.A. (1974) *General Viticulture*. University of California Press, Berkeley & Los Angeles, California.

Xuéreb, A. & Thiéry, D. (2006) Does natural larval parasitism of *Lobesia botrana* (Lepidoptera: Tortricidae) vary between years, generation, density of the host and vine cultivar? *Bulletin of Entomological Research*, **96**, 105–110.

Appendix: Brief overview of the *L. botrana* dynamics model

The biology of grape and *L. botrana* is embedded in an Erlang distributed maturation time demographic model that simulates the dynamics of age-structured populations (Manetsch, 1976; Vansickle, 1977; DiCola *et al.*, 1999: 523–524). The general time invariant model for the *i*th age class of a population is implemented in discrete form (Eqn (A1)).

$$\frac{dN_i}{dt} = \frac{k\,\Delta x}{\Delta}\left[N_{i-1}(t) - N_i(t)\right] - \mu_i(t)\,N_i(t). \quad (A1)$$

where N_i is the abundance of the *i*th age class in number or mass units, dt is the change in time (a day), k is the number of age classes, Δ in degree days is the expected mean developmental time, Δx is a daily increment of physiological age computed using the nonlinear model (text Eqns (2i–ii)) and $\mu_i(t)$ is the age-specific proportional net loss rate (+, −) of births as modified by temperature and nutrition (text), the death rate of all stages as a result of temperature (μ_T) and composite mortality of eggs-larvae (μ_c) (see text). The distribution of final maturation times of a cohort is determined by the number of age classes (k), the mean maturation time Δ and the variance (*var*) of maturation times ($k = \Delta^2/\text{var}$) (Fig. A1a, b). The larger the value of k, the narrower the Erlang distribution of developmental times. We chose a value of $k = 25$ as a rough estimate to simulate the emergence of adults from diapause pupae (see text).

A time varying form of the model is used in the present study for the larval and pupal stages because Δ for them varies during the season on a daily basis as a result of nutrition (Vansickle, 1977).

All life stages can be included in one dynamics model with eggs, produced by the adult age classes entering the first age cohort [$N_1(t)$] as $x_0(t)$ and the survivors exiting at maximum age as $y(t)$ (Fig. A1a). The flow rates [$r_i(t)$] between age classes depends on the number of age classes k and the numbers of individuals in the previous age class, as well as Δ and Δx.
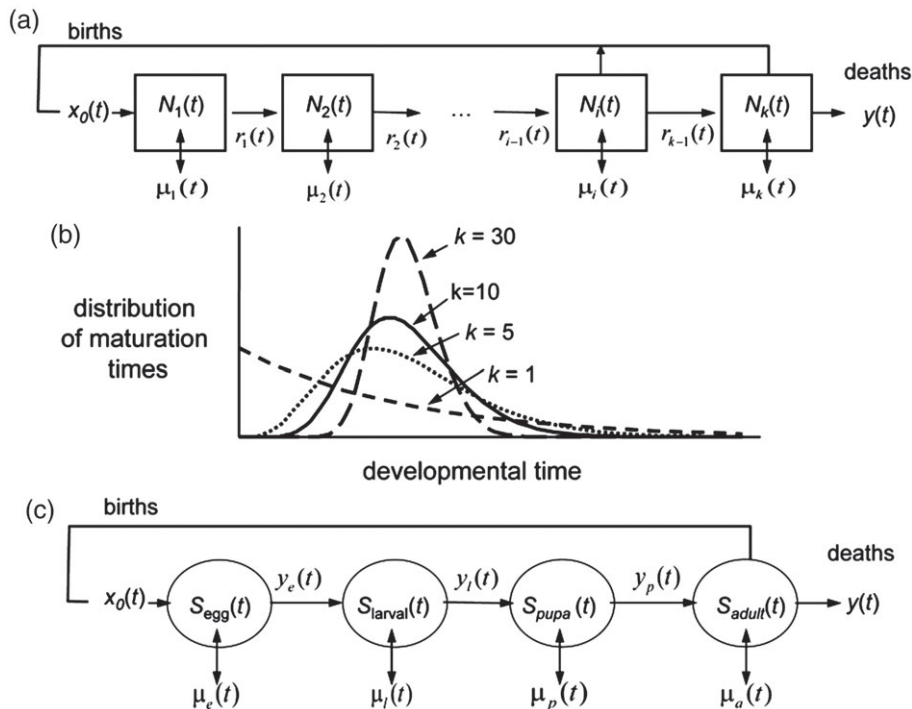

Figure A1 A distributed maturation time model. (a) The general model across all life stages, (b) the stylized distribution of cohort maturation times given different values of the Erlang parameter k and (c) the general model with the dynamics of Fig. A1(a) specified for each life stage, including the stage specific responses to biotic and abiotic factors.

Alternately, as in the present study, separate models may be used for the different stages (S, $i = egg, larval, pupa, adult$) each having stage-specific (subscript s) characteristics (e.g. Δ_s, R_s k_s, ...) with the outflow of the last age class [$y_s(t)$] of a stage [$S_{i,y}(t)$] entering the first age class of the next stage [$S_{i+1, 1}(t)$] and all eggs produced by the adult stage entering the first age class of eggs as $x_0(t)$ (Fig. A1c). The model parameters are listed in Table 1.

The functional response

The number of eggs [$E(t)$] successfully deposited by all females N of age ($x = 0 - max$) is computed using a supply–demand functional response model (Gutierrez & Baumgärtner, 1984) (Eqn (A2)):

$$E(t) = D(t) \left(1 - e^{\frac{-\alpha H(t)}{D(t)}}\right), \tag{A2}$$

where $D(t)$ is the number of eggs that may be deposited by all females (N) (i.e. the demand), H is the number of oviposition sites (supply; the grape clusters predicted by the vine model) and $\alpha = 0.6$ is the search rate.

$$D(t) = sr \sum_{x=0}^{max} f\left(x, T(t), frt_l\right) N(x,t) \tag{A3}$$

The components of $D(t)$ include age-specific per capita fecundity ($f(x, T(t), frt_l)$) as a function of age x, temperature T and larval feeding on fruit stage (frt_l) that produced the adult $N(x,t)$ and sr is the sex ratio (i.e. 0.5).